Italian Journal of Zoology

ISSN: 1125-0003 (Print) 1748-5851 (Online) Journal homepage: http://www.tandfonline.com/loi/tizo20

Cryptic diversity in a chirally variable land snail

M. V. Modica, P. Colangelo, A. Hallgass, A. Barco & M. Oliverio

To cite this article: M. V. Modica, P. Colangelo, A. Hallgass, A. Barco & M. Oliverio (2016): Cryptic diversity in a chirally variable land snail, Italian Journal of Zoology, DOI: 10.1080/11250003.2016.1186234

To link to this article: http://dx.doi.org/10.1080/11250003.2016.1186234

Published online: 26 May 2016.

Italian Journal of Zoology, 2016, 1–13
http://dx.doi.org/10.1080/11250003.2016.1186234

Taylor & Francis
Taylor & Francis Group

Cryptic diversity in a chirally variable land snail

M. V. MODICA[1]*, P. COLANGELO[2], A. HALLGASS[3], A. BARCO[4], & M. OLIVERIO[1]

[1]*Department of Biology and Biotechnologies "Charles Darwin", Sapienza University of Roma, Italy,* [2]*National Research Council, Institute of Ecosystem Study, Verbania Pallanza, Italy,* [3]*Via della Divina Provvidenza, Roma, Italy, and* [4]*GEOMAR, Helmoltz Centre for Ocean Research Kiel, Kiel, Germany*

(Received 14 December 2015; accepted 18 April 2016)

Abstract
Jaminia quadridens (Mollusca: Gastropoda: Heterobranchia: Pulmonata: Stylommatophora: Enidae) is a land snail living up to 2400 m above sea level on calcareous meadow slopes. It is widely distributed in Central and Southern Europe, with two subspecies currently recognised (*J. quadridens quadridens* and *J. quadridens elongata*). Like other Enidae, the genus *Jaminia* is sinistrally coiled, whilst the vast majority of gastropods are dextral. Chirality in snails is determined in the early embryonic stages by a single gene with maternal effect. Following the discovery of reversed (dextral) populations in Abruzzi, we investigated the genetic variability of *Jaminia quadridens* in central and southern Italy. In fact, reversal of chirality is often associated with extremely rapid speciation in snails ("single gene speciation"), as gene flow between opposite chiral morphs can be severely reduced by pre-copula isolation mechanisms. Phylogenetic analyses with different inference methods, haplotype analyses and species delimitation analyses were carried out on cytochtome oxydase subunit I (COI) sequences of 126 *Jaminia* specimens from central and southern Italy, Sardinia and Provence. Our results suggested a complex framework, with at least five lineages that may represent distinct species, in agreement with biogeographic patterns previously reported for other terrestrial taxa. Southern populations of an ancestral stock probably underwent allopatric speciation while surviving in glacial refugia during the Pleistocene. Colonization of central Italy may be recent, with evidences of current gene flow between populations of a single species, which includes reversed individuals. The appearance of chiral reversal was statistically associated with marginal demes but apparently not related to other biological, ecological or historical factors. As land snails are generally severely affected by habitat degradation, due to their ecological requirements, our results have important implications for conservation. *J. quadridens* in Italy may comprise a complex of distinct species, mostly with restricted ranges, which may suffer from environmental changes more than a single, widely distributed species would.

Keywords: Jaminia, *chirality*, *COI*, *species delimitation*

Introduction

The genus *Jaminia* Risso, 1826, comprises pulmonate land snails of the family Enidae with a South European chorotype (Vigna Taglianti et al. 1992). The type species of the genus, *Jaminia quadridens* (O. F. Müller, 1774) is reported to be widely distributed in Europe, ranging from Spain to central Germany, peninsular Italy and northern Greece. Fauna Europaea (Bank 2013) recognises two subspecies: *Jamina quadridens quadridens* and *J. quadridens elongata* (Moquin-Tandon, 1856), the latter characterised by a slender shell and apparently replacing the nominal subspecies in Spain, southern France and northern Italy, from East Rhone to Maritime Alps including northern Corsica.

Jaminia quadridens lives on meadow slopes and poriferous calcareous soils and can be found up to 2400 m above sea level (asl) in the Alps, often on sheep and goat pastures. It is sensitive to both overgrazing from livestock and invasion of other vegetation, as these factors can cause the loss of its grassland habitat; even if the population size of the species is currently not known, a certain degree of decline was reported in the edge population, according to the International Union for the Conservation of Nature (IUCN 2015). Due to its putative wide range, it is indicated as of Least Concern (LC) in the IUCN Red List of Threatened Species.

*Correspondence: Maria Vittoria Modica, Department of Biology and Biotechnologies "Charles Darwin", Sapienza University, Viale dell'Università 32, Roma 00185, Italy. Tel: +39 0649914307. Fax: +39 064958259. Email: mariavittoria.modica@uniroma1.it

As in the other two currently known species of *Jaminia*, i.e. *J. loewi* (Philippi, 1844) and *J. thiesseana* (Westerlund & Blanc, 1879), both with an East-Mediterranean chorotype (Vigna Taglianti et al. 1992), the shell is sinistrally coiled, an unusual condition for gastropods. Coil direction is related to chirality in snails, which in turn is a textbook example of maternal effect (or delayed maternal inheritance), with the genotype of the mother determining the phenotype of the offspring (Boycott & Diver 1923; Sturtevant 1923; Schilthuizen & Davison 2005). In fact, direction of chirality in snails relies on the polar orientation of cells during early embryonic stages, which has been demonstrated to depend on a maternally inherited dominant cytoplasmic factor probably encoded by a single gene (Sturtevant 1923; Degner 1952; Asami et al. 2008). This gene with maternal effect (or delayed inheritance) is responsible for an asymmetric blastomere cleavage, which dictates at later larval stages an asymmetric expression of other downstream genes, which ultimately affects dextral–sinistral asymmetry (Harada et al. 2004; Hierck et al. 2005; Kuroda et al. 2009; Shimizu et al. 2011, 2013; Liu et al. 2013; Kuroda 2014). This signalling cascade involves the expression of *nodal*, a gene involved in chirality in mammals and molluscs (Grande & Patel 2009), suggesting that the whole symmetry-breaking cascade (back to the maternal-effect gene) may be conserved across phyla (Oliverio et al. 2010): the latter hypothesis seems confirmed by the very recent discovery that a diaphanous-related *formin* gene is perfectly associated with symmetry breaking in the pond snail *Lymnaea* and affects chirality in the frog *Xenopus* (Davison et al. 2016).

Most snails are dextral, but reversed chirality has been observed at different taxonomic levels in gastropods. Dextral species can present rare reversed individuals or small populations with frequent or uniform sinistrality. There are also several species, genera or even families of gastropods with dominant sinistrality (Davison et al. 2005). *Jaminia* is one such sinistral taxon. However, we observed a reversal to dextral chirality in three locally uniform populations found above 1700 m asl in central Italy. Within these dextral populations we have never sampled or observed normal sinistral individuals, which instead are found at lower elevations.

Mutations in the maternal-effect chirality gene have been claimed to be involved in single-gene speciation events in snails (Ueshima & Asami 2003). In fact, reproduction of reverse-coiled individuals is usually hampered due to reverse anatomical organization of genital organs and even mirrored courtship behaviour (Gittenberger 1988; Schilthuizen & Davison 2005; Davison et al. 2009; Asami et al. 2011; Koene & Cosijn 2012; Schilthuizen et al. 2012). Due to frequency-dependent selection by the non-reversed individuals, the reversed morph tends to disappear from the populations. However, the reduction of gene flow between chiral morphs may give rise to a new reversed species in the presence of other mechanisms that stabilise the reversed morph, such as genetic drift in a small population, or selective pressures as described in *Sasuma* snails (Hoso et al. 2010). The chirality gene was thus included in the so-called "magic traits" whose mutations can dramatically increase the pace of speciation processes (Servedio et al. 2011).

In the present research we aimed to study the genetic diversity of Italian populations of *Jaminia quadridens*, including three populations representative of the reversed morph. Additionally, we aimed at assessing whether the dextral morphs represent a distinct monophyletic lineage(s). We used a DNA-barcoding approach to investigate the genetic variation at the mitochondrial gene for the COI and evaluate the possible occurrence of cryptic species within *Jaminia quadridens*. Furthermore, to better understand the origin of the reverse morph, we performed a population-scale investigation. Additionally, we used a generalised linear model (GLM) to test the influence of environmental factors on the occurrence of opposite chiral morphs.

Material and methods

Specimen collection

A total number of 124 live specimens, morphologically ascribed to *Jaminia quadridens quadridens*, were collected at 19 sites in central and southern Italy and in Sardinia (Table I; Figure 1), including specimens from a locality (Prato, Florence) within the area reported in the original description of the species. Two specimens morphologically ascribed to *Jaminia quadridens elongata* from Provence Alps were included in the analyses. All sampled material was preserved in 100% ethanol and deposited in the Malacological collections of the Department of Biology and Biotechnologies "Charles Darwin" (Sapienza University of Roma) and of the Muséum National d'Histoire Naturelle (Paris). An additional 20 sites in central Italy were sampled for the presence of empty shells of both chiral morphs, and presence data of the chirally reversed morph were used in the analysis of environmental factors influencing its distribution (see below; Supplemental Table I).

Table I. Material included in the molecular analyses. Voucher numbers, collection data, chirality and COI sequences accession numbers of European Molecular Biology Laboratory.

Voucher no.	Locality	Chirality	Accession no.
BAU01427.01	Monte Genzana, Italy 41.928513° 13.880825° 1401 m	Sinistral	LT549484
BAU01427.03	Monte Genzana, Italy 41.928513° 13.880825° 1401 m	Sinistral	LT549485
BAU01428.01	Monte Genzana, Italy 41.925442° 13.915955° 1819 m	Dextral	LT549486
BAU01428.02	Monte Genzana, Italy 41.925442° 13.915955° 1819 m	Dextral	LT549487
BAU01428.03	Monte Genzana, Italy 41.925442° 13.915955° 1819 m	Dextral	LT549488
BAU01428.04	Monte Genzana, Italy 41.925442° 13.915955° 1819 m	Dextral	LT549489
BAU01428.06	Monte Genzana, Italy 41.925442° 13.915955° 1819 m	Dextral	LT549490
BAU01428.07	Monte Genzana, Italy 41.925442° 13.915955° 1819 m	Dextral	LT549491
BAU01428.08	Monte Genzana, Italy 41.925442° 13.915955° 1819 m	Dextral	LT549492
BAU01429.01	Monte Genzana, Italy 41.921817° 13.915342° 1724 m	Sinistral	LT549493
BAU01429.02	Monte Genzana, Italy 41.921817° 13.915342° 1724 m	Sinistral	LT549494
BAU01429.03	Monte Genzana, Italy 41.921817° 13.915342° 1724 m	Sinistral	LT549495
BAU01430.01	Monte Genzana, Italy 41.921817° 13.915342° 1724 m	Sinistral	LT549496
BAU01430.02	Monte Genzana, Italy 41.921817° 13.915342° 1724 m	Sinistral	LT549497
BAU01431.01	Lago Matese, Italy 41.4225° 14.406944° 1146 m	Sinistral	LT549498
BAU01431.02	Lago Matese, Italy 41.4225° 14.406944° 1146 m	Sinistral	LT549499
BAU01431.03	Lago Matese, Italy 41.4225° 14.406944° 1146 m	Sinistral	LT549500
BAU01431.04	Lago Matese, Italy 41.4225° 14.406944° 1146 m	Sinistral	LT549501
BAU01432.01	Prati di mezzo, Italy 41.660610° 13.924484° 1446 m	Dextral	LT549502
BAU01432.02	Prati di mezzo, Italy 41.660610° 13.924484° 1446 m	Dextral	LT549503
BAU01432.03	Prati di mezzo, Italy 41.660610° 13.924484° 1446 m	Dextral	LT549504
BAU01432.04	Prati di mezzo, Italy 41.660610° 13.924484° 1446 m	Dextral	LT549505
BAU01432.05	Prati di mezzo, Italy 41.660610° 13.924484° 1446 m	Dextral	LT549506
BAU01432.06	Prati di mezzo, Italy 41.660610° 13.924484° 1446 m	Dextral	LT549507
BAU01432.07	Prati di mezzo, Italy 41.660610° 13.924484° 1446 m	Dextral	LT549508
BAU01432.08	Prati di mezzo, Italy 41.660610° 13.924484° 1446 m	Dextral	LT549509
BAU01432.11	Prati di mezzo, Italy 41.660610° 13.924484° 1446 m	Dextral	LT549510
BAU01433.01	Settefrati, Italy 41.668619° 13.868687° 1032 m	Sinistral	LT549511
BAU01433.02	Settefrati, Italy 41.668619° 13.868687° 1032 m	Sinistral	LT549512
BAU01433.03	Settefrati, Italy 41.668619° 13.868687° 1032 m	Sinistral	LT549513
BAU01434.02	Terminio, Italy 40.848330° 14.989442° 1005 m	Sinistral	LT549514
BAU01434.03	Terminio, Italy 40.848330° 14.989442° 1005 m	Sinistral	LT549515
BAU01434.04	Terminio, Italy 40.848330° 14.989442° 1005 m	Sinistral	LT549516
BAU01434.06	Terminio, Italy 40.848330° 14.989442° 1005 m	Sinistral	LT549517
BAU01434.07	Terminio, Italy 40.848330° 14.989442° 1005 m	Sinistral	LT549518
BAU01434.08	Terminio, Italy 40.848330° 14.989442° 1005 m	Sinistral	LT549519
BAU01435.01	Gargano, Italy 41.683611° 15.660278° 541 m	Sinistral	LT549520
BAU01435.02	Gargano, Italy 41.683611° 15.660278° 541 m	Sinistral	LT549521
BAU01435.03	Gargano, Italy 41.683611° 15.660278° 541 m	Sinistral	LT549522
BAU01435.04	Gargano, Italy 41.683611° 15.660278° 541 m	Sinistral	LT549523
BAU01435.05	Gargano, Italy 41.683611° 15.660278° 541 m	Sinistral	LT549524
BAU01436.02	Monte Autore, Italy 41.954722° 13.203333° 1750 m	Sinistral	LT549525
BAU01436.03	Monte Autore, Italy 41.954722° 13.203333° 1750 m	Sinistral	LT549526
BAU01436.04	Monte Autore, Italy 41.954722° 13.203333° 1750 m	Sinistral	LT549527
BAU01436.05	Monte Autore, Italy 41.954722° 13.203333° 1750 m	Sinistral	LT549528
BAU01437.01	Monte Gennaro, Italy 42.042035° 12.830991° 881 m	Sinistral	LT549529
BAU01437.02	Monte Gennaro, Italy 42.042035° 12.830991° 881 m	Sinistral	LT549530
BAU01437.04	Monte Gennaro, Italy 42.042035° 12.830991° 881 m	Sinistral	LT549531
BAU01437.07	Monte Gennaro, Italy 42.042035° 12.830991° 881 m	Sinistral	LT549532
BAU01438.01	Monte Cucco, Italy 43.350960° 12.767310° 1122 m	Sinistral	LT549533
BAU01438.03	Monte Cucco, Italy 43.350960° 12.767310° 1122 m	Sinistral	LT549534
BAU01438.04	Monte Cucco, Italy 43.350960° 12.767310° 1122 m	Sinistral	LT549535
BAU01438.05	Monte Cucco, Italy 43.350960° 12.767310° 1122 m	Sinistral	LT549536
BAU01438.06	Monte Cucco, Italy 43.350960° 12.767310° 1122 m	Sinistral	LT549537
BAU01438.07	Monte Cucco, Italy 43.350960° 12.767310° 1122 m	Sinistral	LT549538
BAU01438.09	Monte Cucco, Italy 43.350960° 12.767310° 1122 m	Sinistral	LT549539
BAU01438.10	Monte Cucco, Italy 43.350960° 12.767310° 1122 m	Sinistral	LT549540
BAU01438.11	Monte Cucco, Italy 43.350960° 12.767310° 1122 m	Sinistral	LT549541
BAU01439.01	Monte Albo, Italy 40.568666° 9.636735° 823 m	Sinistral	LT549542

(*Continued*)

Table I. (Continued).

Voucher no.	Locality	Chirality	Accession no.
BAU01439.06	Monte Albo, Italy 40.568666° 9.636735° 823 m	Sinistral	LT549543
BAU01439.07	Monte Albo, Italy 40.568666° 9.636735° 823 m	Sinistral	LT549544
BAU01439.08	Monte Albo, Italy 40.568666° 9.636735° 823 m	Sinistral	LT549545
BAU01439.09	Monte Albo, Italy 40.568666° 9.636735° 823 m	Sinistral	LT549546
BAU01440.01	Alpes-des-Haute-Provence, France 44.1203° 6,633755° 1561 m	Sinistral	LT549547
BAU01440.02	Alpes-des-Haute-Provence, France 44.1203° 6,633755° 1561 m	Sinistral	LT549548
BAU01441.01	Aremogna, Italy 41.829722° 14.009444° 1850 m	Dextral	LT549549
BAU01441.02	Aremogna, Italy 41.829722° 14.009444° 1850 m	Dextral	LT549550
BAU01441.03	Aremogna, Italy 41.829722° 14.009444° 1850 m	Dextral	LT549551
BAU01441.04	Aremogna, Italy 41.829722° 14.009444° 1850 m	Dextral	LT549552
BAU01441.05	Aremogna, Italy 41.829722° 14.009444° 1850 m	Dextral	LT549553
BAU01442.02	Monte Torre Maggiore, Italy 42.661389° 12.588056° 770 m	Sinistral	LT549554
BAU01442.03	Monte Torre Maggiore, Italy 42.661389° 12.588056° 770 m	Sinistral	LT549555
BAU01442.04	Monte Torre Maggiore, Italy 42.661389° 12.588056° 770 m	Sinistral	LT549556
BAU01443.01	Rocca Pia, Italy 41.919722° 13.978611° 1280 m	Sinistral	LT549557
BAU01443.02	Rocca Pia, Italy 41.919722° 13.978611° 1280 m	Sinistral	LT549558
BAU01443.04	Rocca Pia, Italy 41.919722° 13.978611° 1280 m	Sinistral	LT549559
BAU01443.06	Rocca Pia, Italy 41.919722° 13.978611° 1280 m	Sinistral	LT549560
BAU01443.07	Rocca Pia, Italy 41.919722° 13.978611° 1280 m	Sinistral	LT549561
BAU01443.08	Rocca Pia, Italy 41.919722° 13.978611° 1280 m	Sinistral	LT549562
BAU01443.09	Rocca Pia, Italy 41.919722° 13.978611° 1280 m	Sinistral	LT549563
BAU01443.10	Rocca Pia, Italy 41.919722° 13.978611° 1280 m	Sinistral	LT549564
BAU01444.01	Pollino, Italy 39.918383° 16.136265° 1560 m	Sinistral	LT549565
BAU01444.03	Pollino, Italy 39.918383° 16.136265° 1560 m	Sinistral	LT549566
BAU01444.04	Pollino, Italy 39.918383° 16.136265° 1560 m	Sinistral	LT549567
BAU01444.05	Pollino, Italy 39.918383° 16.136265° 1560 m	Sinistral	LT549568
BAU01444.06	Pollino, Italy 39.918383° 16.136265° 1560 m	Sinistral	LT549569
BAU01444.07	Pollino, Italy 39.918383° 16.136265° 1560 m	Sinistral	LT549570
BAU01444.09	Pollino, Italy 39.918383° 16.136265° 1560 m	Sinistral	LT549571
BAU01445.01	Laga, Italy 42.689722° 13.293056° 1280 m	Sinistral	LT549572
BAU01445.03	Laga, Italy 42.689722° 13.293056° 1280 m	Sinistral	LT549573
BAU01445.04	Laga, Italy 42.689722° 13.293056° 1280 m	Sinistral	LT549574
BAU01445.05	Laga, Italy 42.689722° 13.293056° 1280 m	Sinistral	LT549575
BAU01445.06	Laga, Italy 42.689722° 13.293056° 1280 m	Sinistral	LT549576
BAU01446.01	Prato, Italy 43.884722° 11.130278° 450 m	Sinistral	LT549577
BAU01446.02	Prato, Italy 43.884722° 11.130278° 450 m	Sinistral	LT549578
BAU01446.03	Prato, Italy 43.884722° 11.130278° 450 m	Sinistral	LT549579
BAU01447.01	Monte Semprevisa, Italy 41.562329° 13.123870° 1112 m	Sinistral	LT549580
BAU01447.02	Monte Semprevisa, Italy 41.562329° 13.123870° 1112 m	Sinistral	LT549581
BAU01447.03	Monte Semprevisa, Italy 41.562329° 13.123870° 1112 m	Sinistral	LT549582
BAU01447.04	Monte Semprevisa, Italy 41.562329° 13.123870° 1112 m	Sinistral	LT549583
BAU01448.01	Monte Petrella, Italy 41.316644° 13.654817° 1280 m	Sinistral	LT549584
BAU01448.02	Monte Petrella, Italy 41.316644° 13.654817° 1280 m	Sinistral	LT549585
BAU01448.03	Monte Petrella, Italy 41.316644° 13.654817° 1280 m	Sinistral	LT549586
BAU01448.04	Monte Petrella, Italy 41.316644° 13.654817° 1280 m	Sinistral	LT549587
BAU01448.05	Monte Petrella, Italy 41.316644° 13.654817° 1280 m	Sinistral	LT549588
BAU01448.06	Monte Petrella, Italy 41.316644° 13.654817° 1280 m	Sinistral	LT549589
BAU01448.07	Monte Petrella, Italy 41.316644° 13.654817° 1280 m	Sinistral	LT549590
BAU01448.08	Monte Petrella, Italy 41.316644° 13.654817° 1280 m	Sinistral	LT549591
BAU01448.09	Monte Petrella, Italy 41.316644° 13.654817° 1280 m	Sinistral	LT549592
BAU01448.10	Monte Petrella, Italy 41.316644° 13.654817° 1280 m	Sinistral	LT549593
BAU01449.02	Monte Petrella, Italy 41.318247° 13.654168° 1274 m	Sinistral	LT549594
BAU01449.03	Monte Petrella, Italy 41.318247° 13.654168° 1274 m	Sinistral	LT549595
BAU01449.04	Monte Petrella, Italy 41.318247° 13.654168° 1274 m	Sinistral	LT549596
BAU01449.05	Monte Petrella, Italy 41.318247° 13.654168° 1274 m	Sinistral	LT549597
BAU01449.06	Monte Petrella, Italy 41.318247° 13.654168° 1274 m	Sinistral	LT549598
BAU01449.07	Monte Petrella, Italy 41.318247° 13.654168° 1274 m	Sinistral	LT549599
BAU01449.08	Monte Petrella, Italy 41.318247° 13.654168° 1274 m	Sinistral	LT549600
BAU01449.09	Monte Petrella, Italy 41.318247° 13.654168° 1274 m	Sinistral	LT549601
BAU01449.10	Monte Petrella, Italy 41.318247° 13.654168° 1274 m	Sinistral	LT549602

(*Continued*)

Table I. (Continued).

Voucher no.	Locality	Chirality	Accession no.
BAU01450.01	Monte Petrella, Italy 41.314563° 13.622863° 1070 m	Sinistral	LT549603
BAU01450.02	Monte Petrella, Italy 41.314563° 13.622863° 1070 m	Sinistral	LT549604
BAU01450.03	Monte Petrella, Italy 41.314563° 13.622863° 1070 m	Sinistral	LT549605
BAU01450.04	Monte Petrella, Italy 41.314563° 13.622863° 1070 m	Sinistral	LT549606
BAU01450.05	Monte Petrella, Italy 41.314563° 13.622863° 1070 m	Sinistral	LT549607
BAU01450.06	Monte Petrella, Italy 41.314563° 13.622863° 1070 m	Sinistral	LT549608
BAU01451.01	Monte Cairo, Italy 41.546634° 13.770514° 1250 m	Sinistral	LT549609

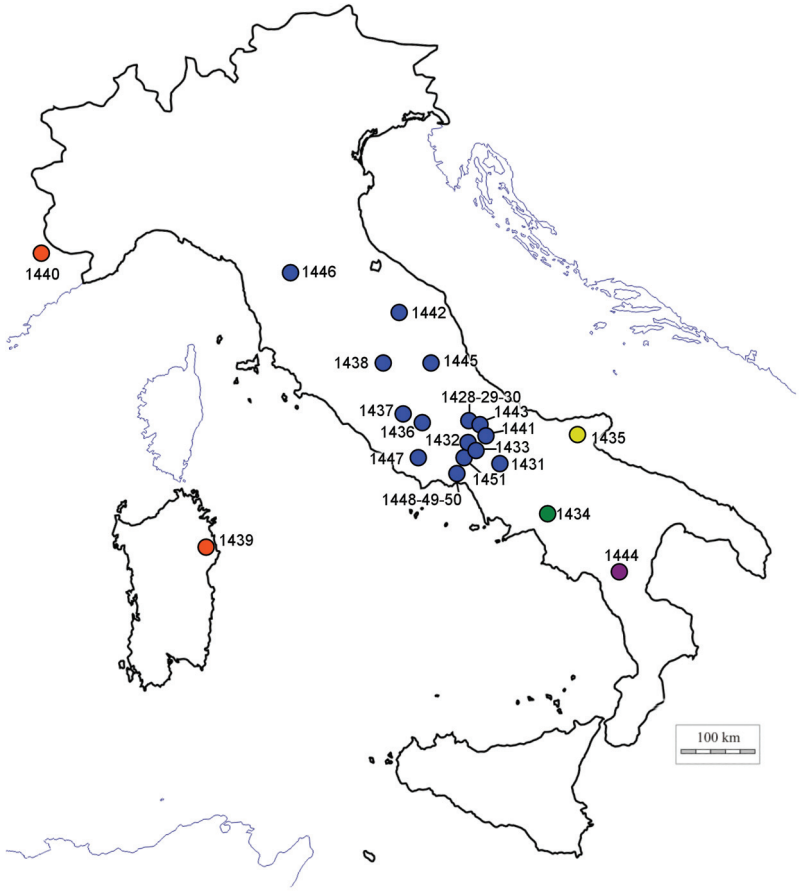

Figure 1. Geographic distribution of the sampling sites. In the online version, colour of the dots reflects the partition into Molecular Operational Taxonomic Units (MOTUs) by ABGD analyses (see also Figure 2).

DNA extraction, PCR amplification and sequencing

Total genomic DNA was extracted using a standard proteinase K – phenol/chloroform method with ethanol precipitation as reported in (Oliverio & Mariottini 2001). The DNA-barcode fragments of the mitochondrial cytochrome oxidase subunit I (COI) was amplified by polymerase chain reaction (PCR) using the universal primers LCO1490 and HCO2198 (Folmer et al. 1994), in 35 amplification cycles (30 seconds at 94°C, 40 seconds at 60°C, 1 minute at 72°C). PCR products were purified with Exosap-IT (USB Corporation) and sequenced by Macrogen Inc. (Seoul, South Korea). All sequence data were deposited in GenBank (accession numbers in Table I).

Phylogenetic analyses and species delimitation

Both forward and reverse DNA sequences were analysed in Geneious 4.6.3 (Biomatters Ltd.) to

complete contigs that were then readily aligned by hand. The invertebrate mitochondrial code table was used to deduce encoded amino acid sequences and check for stop codons. Alignments are available upon request to the authors.

Base composition of nucleotide sequences was analysed with MEGA 5.0 (Tamura et al. 2011). Nucleotide homogeneity was tested with the χ^2 statistics implemented in PAUP* v. 4.0b10 (Swofford 1993).

Species delimitation was based on the identification of Molecular Operational Taxonomic Units (MOTUs), subsequently tested as species hypotheses in a phylogenetic framework (reciprocal monophyly of MOTUs). The two distinct and complementary methods employed to identify MOTUs in our data set were: (1) the Automatic Barcode Gap Discovery (ABGD), and (2) the General Mixed Yule Coalescent Method (GMYC). (1) The ABGD method (Puillandre et al. 2012a) statistically infers the barcode gap in a molecular distance matrix, and accordingly partitions the sequences into putative species. This procedure is recursively applied to the obtained partitions, to check for internal splitting. ABGD was carried out using the ABGD web server (at wwwabi.snv.jussieu.fr/public/abgd/abgdweb.html) with the default settings. Genetic distances were estimated with the Kimura two-parameter model (K2p). Although the suitability of this model of nucleotide evolution in DNA-barcoding studies is debated (Srivathsan & Meier 2011), further studies have highlighted that, especially at low divergence values, the difference between results obtained with non-calibrated (p) distances and with more complex models is extremely reduced (Collins et al. 2012). Here, we retain the K2p due to its widespread use in barcoding analyses. (2) GMYC (Pons et al. 2006) uses the differences of the branching rates in an ultrametric phylogenetic tree to distinguish between inter- and intraspecific branching events, and thus determine species boundaries. The switch from speciation to coalescence can be supposed to be unique (in the single-threshold GMYC method: Pons et al. 2006), or the first species partition can be recursively re-analysed to further split or join species (multiple-threshold GMYC method: Monaghan et al. 2009). An ultrametric tree was generated in BEAST v. 1.7.5 (Drummond & Rambaut 2007). Identical haplotypes, which are problematic for GMYC (Monaghan et al. 2009; Tanzler et al. 2012), were removed from our data set using the option Collapse in the ALTER web server (Glez-Pena et al. 2010; available at http://sing.ei.uvigo.es/ALTER/) resulting in a data set of 39 ingroup sequences. Two relaxed log-normal clock analyses were conducted with a Coalescent tree prior, identified as the best-fitting parameters to be used with the GMYC (Monaghan et al. 2009). The two MCMC chains were run for 100,000,000 generations and sampled every 1000 trees, until convergence was achieved as confirmed by the inspection of the effective sample size in TRACER v. 1.6 (Rambaut et al. 2014). The consensus tree obtained was used to infer species delimitation with the GMYC method, using both the single- and the multiple-threshold methods, with the package SPLITS (Ezard et al. 2009) in R (R Development Core Team 2014).

Phylogenetic trees were inferred by maximum likelihood (ML) and Bayesian inference (BI), using a sequence of the closely related *Ena montana* as outgroup (accession number JX911299). Appropriate models of nucleotide substitution were selected by ModelTest (Posada & Crandall 1998, 2001) and MrModelTest v. 2.2 (Nylander 2004), in conjunction with PAUP v. 4.0b10 (Swofford 2002), using the Akaike information criterion (AIC). ML phylogeny was constructed using PHyML 3.0 (Guindon & Gascuel 2003) with the substitution model selected in ModelTest. Four substitution rate categories were considered, while gamma shape parameters, transition/transversion ratios, nucleotide frequencies and proportion of invariable sites were estimated from the data. BI trees were constructed with MrBayes v. 3.1.2 (Ronquist et al. 2012) running a four-chain Metropolis-coupled Markov chain Monte Carlo for 10^7 generations; trees were sampled every 1000 generation, and used to build consensus trees after a 25% burn-in. Convergence of the runs was assessed using the standard deviation of the split frequencies and examining the log likelihood values of the cold chain.

Phylogeographic analysis

To investigate the structuring of intra-clade genetic diversity, we reconstructed the relationships among haplotypes, using the statistical parsimony network analysis implemented in PEGAS (Paradis 2010). Furthermore, for each MOTU confidently tested as a reliable species hypothesis by the species delimitation approach, the genetic diversity (nucleotide diversity, haplotype diversity and nucleotide differences) was evaluated with the software DnaSP (Librado & Rozas 2009).

Under a model of isolation by distance (IBD), the genetic distance between populations is expected to increase with geographical distance. Here, we tested whether an IBD model could explain the genetic structure observed in the central Italy clade E using

a Mantel test as implemented in the R package VEGAN (Oksanen et al. 2012). The significance of the Mantel test was assessed using a permutation procedure with 10,000 replications.

Environmental factors

We used a GLM to explicitly test the influence of environmental factors on the chiral reversal of *Jaminia quadridens* land snails. In particular, we focused on the possibility that spatial and/or ecological constraints might produce conditions that could reduce the negative selection pressure on reversed morphs. Indeed, in sub-optimal ecological conditions or in marginal populations, where population density is low, the chance to fix the chiral reversal in small demes becomes higher. Given that *Jaminia* is a mountain species, elevation was used as a variable related to the spatial distribution of inverse chiral morphs on an altitudinal gradient. Furthermore, snails are severely constrained by precipitation and humidity, and the rare dextral morph might be less disadvantageous in low-density populations occurring in areas characterised by sub-optimal conditions of rainfall across the year. According to this consideration, we included in the GLM analysis the rainfall pattern observed at each collecting site as variable related optimal/sub-optimal conditions. The rainfall pattern was obtained by performing a principal component analysis (PCA) on a matrix including eight bioclimatic variables: annual precipitation, precipitation of the wettest month, precipitation of the driest month, precipitation seasonality, precipitation of the wettest quarter, precipitation of driest quarter, precipitation of the warmest quarter and precipitation of the coldest quarter. This approach allowed a reduction of the number of variables and offered a solution to the autocorrelation issues often observed when dealing with bioclimatic variables. The eight tested bioclimatic variables were obtained by raster maps with a resolution of 30 arc-seconds (~1 km) from the WorldClim database (Hijmans et al. 2005; www.worldclim.org). Subsequently, the elevation and the first principal component (PC) axis score (representing the rainfall pattern) were used to fit the GLM models where chirality inversion was coded as a binomial variable (presence/absence). A full model that does not consider the interactions between the two variables was built. Then, we calculated two reduced models (excluding one of the two independent variables in turn) and a null model. Finally, we evaluated the best model using AIC. Analyses (PCA and GLM) were performed using the R statistical environment (R Core Team 2014).

Results

Phylogenetic analysis

A total of 628 bp were unambiguously aligned, without gaps, with 100 variable positions, resulting in 39 distinct haplotypes.

The best-fit model selected both in Modeltest and in MrModeltest according to the AIC was the HKY +I + G; this model was used in ML and BI inference, while values of parameters were estimated during the analyses.

Phylogenetic trees obtained with ML and Bayesian methods did not disagree substantially, being nearly identical at the deepest nodes, and displaying slight differences only in the internal nesting of the most apical clades. The ML phylogenetic tree represented in Figure 2 comprised five major well-supported clades, referred to from here on as MOTUs A–E.

MOTU A included all the Sardinian specimens, and the specimens from Provence Alps putatively ascribed to *Jaminia quadridens elongata*. MOTUs B, C and D corresponded to three southern Italy populations, from Pollino, Gargano and Campania, respectively. Specimens included in MOTU E were all from central Italy, mostly from Abruzzi and Latium, and including Tuscany specimens from Prato. A clear geographic pattern was missing in MOTU E, with specimens from the same sampling sites or localities often not grouped monophyletically. However, MOTU E included a monophyletic terminal lineage (clade E1). Dextral specimens of *Jaminia* were all included in clade E1 but did not form a monophyletic lineage, nor did they appear to be genetically differentiated from sinistral specimens at the mitochondrial marker sequenced.

Species delimitation

ABGD partitioned sequences applying several *a priori* thresholds to the distribution of pairwise genetic distances, and potentially retrieving variable numbers of clusters. Our samples were grouped into five groups with all of the intermediate threshold values used (Figure 2). These groups corresponded to the five main monophyletic lineages retrieved in the ML phylogeny.

Both the single- and multiple-threshold GMYC methods had likelihood values ($L_{GMYCsingle}$ = 258.35 and $L_{GMYCmultiple}$ = 260.32) significantly higher than the likelihood of the null model (L_0 = 34.10, P-value = 0). However, the results of the two methods were not identical, with 16 groups for the single

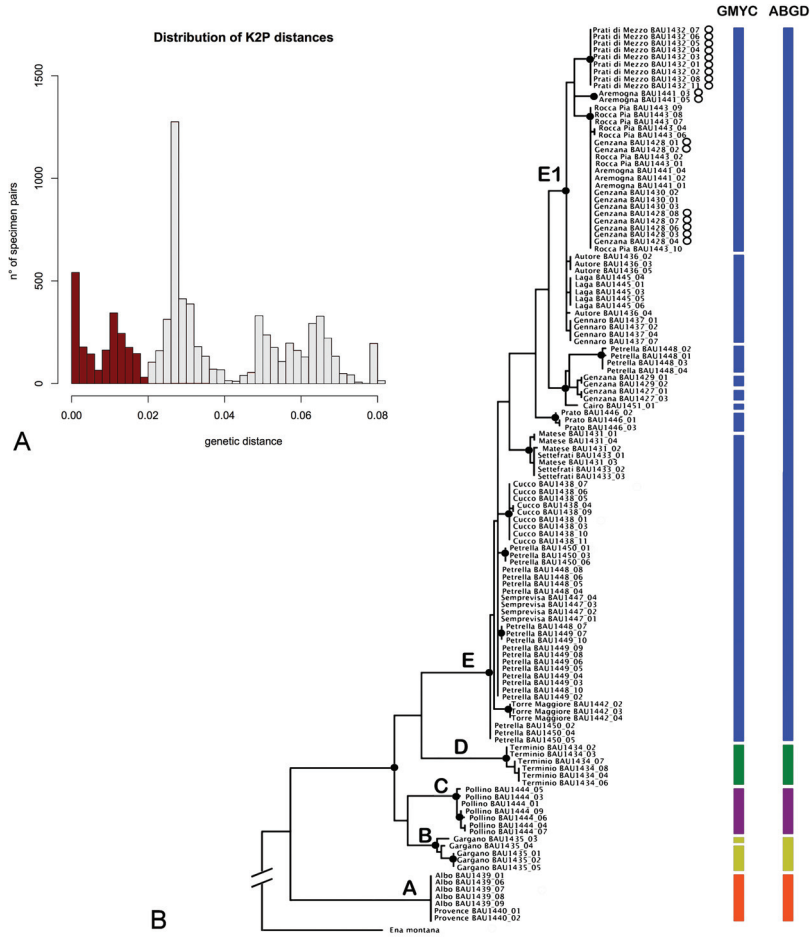

Figure 2. (a) Frequency distribution of the pairwise estimated genetic distances with the Kimura two-parameter (K2p) substitution model. Intra- and inter-MOTU genetic distances are reported respectively in colour and white. (b) Maximum likelihood (ML) phylogenetic tree of the *Jaminia* COI sequences. Vertical bars represent species partitions obtained with GMYC and ABGD methods. Closed circles at nodes indicate high bootstrap support and posterior probability values (bootstrap ≥ 90, PP ≥95). The open circles at the tips indicate dextral specimens (see also Figure 3).

threshold (confidence limits 2–38) and 12 groups for the multiple thresholds (confidence limits: 6–18) (Figure 2). The difference between the two models relied on the internal splitting of clade E (which was recognised as a single unit by ABGD), by defining seven groups in the multiple-threshold and 11 in the single-threshold model. The other groups were identical under both GMYC methods: two of them corresponded to subclades of clade C, while the remaining four corresponded to the other lineages recognised by ABGD.

Mean between-group and within-group K2p distances were calculated in MEGA for the main MOTUs defined by ABGD (A–E). Between-group distances ranged from a maximum value of 0.077 to a minimum value of 0.033, while within-group distances ranged between 0 and 0.02 (Table II). A histogram of the distribution of the pairwise estimated K2p distances is shown in Figure 2. There was no clear gap in the distribution, although two sharp minima were found (at c. 0.002 and c. 0.004).

Table II. Diversity indexes. The number of specimens (N), the number of haplotypes (h), the haplotype (Hd) and the nucleotide (π) diversity were reported for each of the main phylogroups.

Group	N	h	Hd	π
A	7	1	0	0
B	7	6	0.952	0.00303
C	5	3	0.700	0.00605
D	6	3	0.733	0.00265
E	101	26	0.922	0.01986

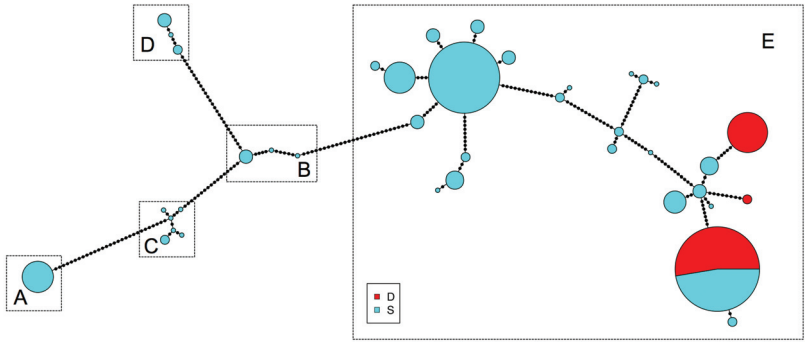

Figure 3. Haplotypes networks for the whole *Jaminia* cytochrome oxydase subunit I (COI) data set. Letters indicate major phyloclades; colours represent chiral morphs (D: dextral; S: sinistral).

Table III. Estimates of evolutionary divergence over sequence pairs. Both between-group and within-group mean values were calculated using the K2p (Kimura 2-parameters) model in MEGA5.

	Clade A	Clade B	Clade C	Clade D	Within group
Clade A					0
Clade B	0.053				0.003
Clade C	0.054	0.033			0.006
Clade D	0.067	0.052	0.048		0.003
Clade E	0.077	0.061	0.058	0.06	0.021

Phylogeographic analysis

The parsimony network analysis recognised, for the total number of 39 haplotypes, five haplogroups consistent with the MOTUs defined by the phylogenetic analysis. However, the five networks were connected with a parsimony threshold < 90%. Haplotypes within the largest haplogroup found, corresponding to clade E, were all connected with a 93% parsimony threshold (Figure 3). Dextral population haplotypes fell all within this last haplogroup.

Haplotype diversity values for each clade ranged from 0 to 0.95, whereas nucleotide diversity ranged from 0 to 0.0197 (Table III).

A scatter plot of K2p genetic distances against geographic distances for clade E is reported in Figure 4. A Mantel test demonstrated the presence of a weak but significant relationship between genetic and geographic distances (r = 0.2; P = 0.002).

Environmental factors

According to AIC, the GLM model considering only the effect of elevation turned out to be the best model (Supplemental Table II). The GLM-estimated coefficients suggest an increase of the probability to find a snail with inverse chirality when the elevation increases (Supplemental Table III). Particularly, the chance to find a snail with inverse chirality exponentially increases after elevation above 1000 m asl (Figure 5).

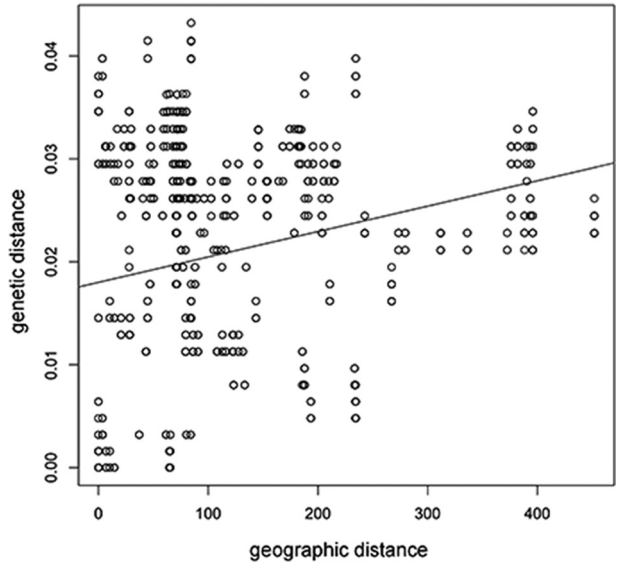

Figure 4. Scatter plot of Kimura two-parameter (K2p) genetic distance versus geographic distance for specimens of the MOTU E.

Discussion

Within our samples, ABGD recognised five partitions corresponding to reciprocally monophyletic haplogroups, while GMYC identified 12 partitions with the multiple-threshold and 16 partitions with the single-threshold model. Remarkably, our result contradicted the pattern commonly observed comparing single- vs multiple-threshold methods, with the latter showing a tendency to overestimate the number of clusters (Monaghan et al. 2009; Puillandre et al.

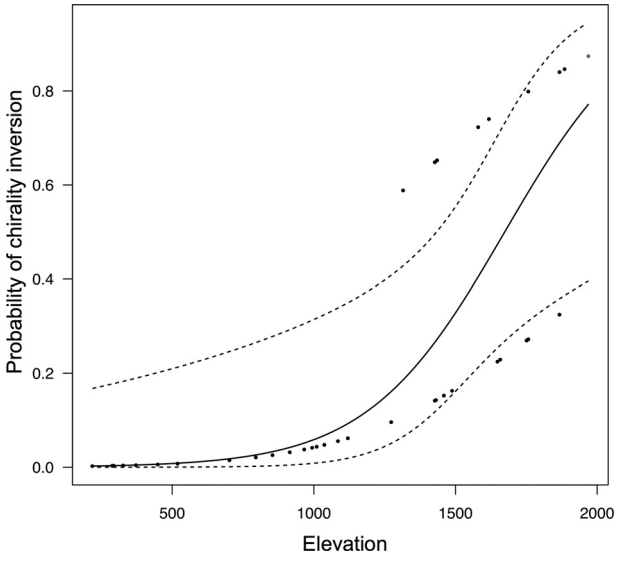

Figure 5. Graph showing the predicted probability of a successful chirality reversal according to the elevation (solid line) based on the generalised linear model (GLM). The dashed lines around the best-fit line indicate a 95% confidence interval. The points plotted on the graph are the partial residuals associated with each value.

2012b; Fujisawa & Barraclough 2013). Here, the multiple-threshold method appeared to yield a more accurate result, as confirmed by the exceedingly broad confidence limits retrieved by GMYC single-threshold method (2–38 groups). This result might be due to the fact that the genetic structure of our sample is better described when the assumptions of the single-threshold method are relaxed (Fujisawa & Barraclough 2013). Most of the splits identified by GMYC corresponded to allopatric subclades of clade E. However, in these conditions GMYC tends to overestimate the number of species (Tanzler et al. 2012), regardless of the threshold method, suggesting that the more conservative ABGD partitioning pattern (five units) may be the most reliable. Furthermore, ABGD partitions are strongly supported by the pattern of COI variation, with nucleotide diversity lower within groups than between groups (Table III). The five MOTUs may represent as many biological species, although the same pattern might also be explained as an ancient mitochondrial divergence in a single species (Tomaz et al. 1996), and needs thus to be supported by other independent sources of data (e.g., nuclear gene sequences or morphological evidences). However, it is noteworthy that very similar geographic structures were observed in other terrestrial gastropod taxa, whose taxonomic status as species complexes was supported by other evidence (Oliverio et al. 1992; Fiorentino et al. 2010), which brings us to propose a multiple species interpretation. One of them, MOTU A (Sardinia and Provence specimens), probably corresponding to a European *Jaminia* stock, is sister to the insular Italy clusters. MOTU A is characterised by an anomalous genetic homogeneity (all specimens sharing exactly the same COI haplotype), which is difficult to explain without more exhaustive sampling in the two areas, but may very likely be attributed to anthropic transportation. The four genetically well-differentiated insular Italy haplogroups (MOTUs B–E) displayed a pattern congruent with the recent biogeographical hypothesis of a refugia-within-refugia scenario, an expansion of the refugia hypothesis of Hewitt (1999, 2000), originally proposed for the Iberian peninsula (Gómez & Lunt 2006). Under this scenario, the isolation in multiple isolated refugia during Pleistocene glacial phases, mainly in the southernmost part of the Italian peninsula, would have prevented gene flow between phylogeographic lineages, leading to high levels of genetic diversity between southern populations (Nieberding et al. 2005; Podnar et al. 2005; Canestrelli et al. 2007). Speciation events in land snails tend to be strictly allopatric, due to the extremely reduced spatial scale of gene flow (e.g. Oliverio et al. 1992; Schilthuizen & Lombaerts 1994; Fiorentino et al. 2010). This effect can be particularly evident in species with peculiar ecological requirements such as *Jaminia*, where isolation of different populations in calcareous mountain habitats could easily lead to divergence, driven by genetic drift.

The central Italy MOTU E (including the Prato sample, broadly topotypic of *Helix quadridens* Müller, 1774), likely corresponds to the nominal *J. quadridens*, and includes also the dextral individuals, which do not form a genetically distinct monophyletic clade. These results suggest that the genetic potential for reversal could have evolved in this amphidromic clade (a clade including both chiral morphs or enantiomorphs), and which, when it occurred, gave rise to groups of dextral individuals possibly establishing as distinct (sub)populations.

Haplotypes belonging to the amphidromic MOTU E, where chiral reversal was observed, displayed relatively high genetic divergences (mean value = 0.021) and evidence of genetic structure. Results of the stratified Mantel test indicated that, as expected, such patterns of genetic divergence are only partially explained by a mechanism of isolation by distance, suggesting that the past occurrence of geographic and/or ecological barriers could have contributed to shaping the genetic structure of the central Italy clade. It is remarkable that the three haplotypes found to carry dextral chirality diverged for a high number of mutations (Figure 3). One of these haplotypes is also shared between opposite chiral morphs. According to these results, chiral

reversal probably arose independently in different populations, also in recent times, and does not reflect the phylogeographic structure of the species. Reversal of chirality, albeit not showing a high frequency, is not rare and was recognised in differed clades of gastropods. Causes of reversal are likely related to mutations in the still unknown chirality gene or along the downstream gene expression pathways (e.g. *Nodal*: Grande & Patel 2009; Kuroda et al. 2009; Liu et al. 2013), but the evolutionary mechanisms leading to the fixation of such mutations are still objects of debate. Interchiral mating in snails is normally impeded or reduced at different degrees, and in a panmictic population the reversed morphs can be negatively selected preventing their persistence in the population. Predation pressures (Hoso et al. 2010) or a strong population structure can counteract the negative selective pressure and allow the fixation of inverse chiral morphs. We tested whether specific conditions, i.e. a sub-optimal rainfall pattern and/or the spatial distribution of populations, triggered favourable conditions for the fixation of an inverse chiral morph. According to GLM, the occurrence of snails with reversed (dextral) chirality, despite not being related to the population genetic structure, was not random. Indeed, the chance to find a snail with inverse chirality increases very rapidly when the elevation is > 1000 m asl. This result suggests that conditions for the fixation of chiral reversal occur only at very high elevations. It is possible that, close to their highest altitudinal limit, populations of *Jaminia* become less dense. Evidence supporting this hypothesis is provided by Baur et al. (2014), who observed a decline in snail abundance with increased altitude in several species of alpine terrestrial gastropods. In small peripheral demes, the likely high level of intra-clutch and thus intra-chiral mating may have triggered the establishment of reversed chiral populations.

In summary, our study highlighted the presence of at least five MOTUs which, pending further testing in an integrative framework by independent evidence (Padial et al. 2010), can be regarded as five distinct species of *Jaminia*. This finding has important implications for biodiversity conservation, as *J. quadridens* is ranked as of "minor concern" in the IUCN Red List of threatened species due to its allegedly wide range. The genus *Jaminia* in Italy is likely to include several species, each of which may be severely affected by habitat degradation or loss, especially given their reduced distribution areas. IUCN Red List category changes due to taxonomic reassessments, often in conjunction with other factors, are not infrequent, especially for less-studied invertebrate taxa.

Acknowledgements

We are grateful to Olivier Gargominy (Muséum National d'Histoire Naturelle, Paris, France) for samples of *Jaminia quadridens elongata* from Provence Alps. Angelo Vannozzi (Roma, Italy) is acknowledged for his collaboration during field collection.

Supplemental data

Supplemental data for this article can be accessed at: http://dx.doi.org/10.1080/11250003.2016.1186234.

References

Asami T, Gittenberger E, Falkner G. 2008. Whole-body enantiomorphy and maternal inheritance of chiral reversal in the pond snail *Lymnaea stagnalis*. Journal of Heredity 99:552–557. DOI:10.1093/jhered/esn032.

Asami T, Utsuno H, van Dooren T, Gittenberger E. 2011. Internal selection against the evolution of left-right reversal. Evolution 65:2399–2411. DOI:10.1111/j.1558-5646.2011.01293.x.

Bank R. 2013. Fauna Europaea: *Jaminia*. Fauna Europaea version 2.6. Available: http://www.faunaeur.org. Accessed Mar 2014 10.

Baur B, Meier T, Baur A, Schmera D. 2014. Terrestrial gastropod diversity in an alpine region: Disentangling effects of elevation, area, geometric constraints, habitat type and land-use intensity. Ecography 37:390–401. DOI:10.1111/ecog.2014.37.issue-4.

Boycott AE, Diver C. 1923. On the inheritance of sinistrality in *Lymnaea peregra*. Proceedings of the Royal Society of London B 95:207–213. DOI:10.1098/rspb.1923.0033.

Canestrelli D, Cimmaruta R, Nascetti G. 2007. Phylogeography and historical demography of the Italian treefrog, *Hyla intermedia*, reveals multiple refugia, population expansions and secondary contacts within peninsular Italy. Molecular Ecology 16:4808–4821. DOI:10.1111/mec.2007.16.issue-22.

Collins RA, Boykin LM, Cruickshank RH, Armstrong KF. 2012. Barcoding's next top model: An evaluation of nucleotide substitution models for specimen identification. Methods in Ecology and Evolution 3:457–465. DOI:10.1111/j.2041-210X.2011.00176.x.

Davison A, Chiba S, Barton NH, Clarke B. 2005. Speciation and gene flow between snails of opposite chirality. PLoS Biology 3:1559–1571. DOI:10.1371/journal.pbio.0030282.

Davison A, Frend HT, Moray C, Wheatley H, Searle LJ, Eichhorn MP. 2009. Mating behaviour in *Lymnaea stagnalis* pond snails is a maternally inherited, lateralized trait. Biology Letters 5:20–22. DOI:10.1098/rsbl.2008.0528.

Davison A, McDowell GS, Holden JM, Johnson HF, Koutsovoulos GD, Liu MM, Hulpiau P, Van Roy F, Wade CM, Banerjee R, Yang F, Chiba S, Davey JW, Jackson DJ, Levin M, Blaxter ML. 2016. Formin is associated with left-right asymmetry in the pond snail and the frog. Current Biology 26:654–660. DOI:10.1016/j.cub.2015.12.071.

Degner E. 1952. Der Erbgang der Inversion bei *Laciniaria biplicata* MTG (Gastr. Pulm.). Mitteilungen aus den Hamburgischen Zoologischen Museum und Institut 51:3–61.

Drummond AJ, Rambaut A. 2007. BEAST: Bayesian evolutionary analysis by sampling trees. BMC Evolutionary Biology 7:214. DOI:10.1186/1471-2148-7-214.

Ezard T, Fujisawa T, Barraclough T. 2009. Splits: SPecies' LImits by threshold statistics. R package.

Fiorentino V, Salomone N, Manganelli G, Giusti F. 2010. Historical biogeography of Tyrrhenian land snails: The *Marmorana-Tyrrheniberus* radiation (Pulmonata, Helicidae). Molecular Phylogenetics and Evolution 55:26–37. DOI:10.1016/j.ympev.2009.11.024.

Folmer O, Black M, Hoeh W, Lutz R, Vrijenhoek R. 1994. DNA primers for amplification of mitochondrial cytochrome c oxidase subunit I from diverse metazoan invertebrates. Molecular Marine Biology and Biotechnology 3:294–299.

Fujisawa T, Barraclough TG. 2013. Delimiting species using single-locus data and the generalized mixed Yule coalescent approach: A revised method and evaluation on simulated data sets. Systematic Biology 62:707–724. DOI:10.1093/sysbio/syt033.

Gittenberger E. 1988. Sympatric speciation in snails: A largely neglected model. Evolution 42:826–828. DOI:10.2307/2408875.

Glez-Pena D, Gomez-Blanco D, Reboiro-Jato M, Fdez-Riverola F, Posada D. 2010. ALTER: Program-oriented conversion of DNA and protein alignments. Nucleic Acids Research 38: W14–18. DOI:10.1093/nar/gkq321.

Gómez A, Lunt DH. 2006. Chapter 5, Refugia within refugia: Patterns of phylogeographic concordance in the Iberian Peninsula. In: Weiss S, Ferrand N, editors. Phylogeography of Southern European refugia. Dordrecht: Springer Verlag. pp. 155–188.

Grande C, Patel NH. 2009. Nodal signalling is involved in left-right asymmetry in snails. Nature 457:1007–1011. DOI:10.1038/nature07603.

Guindon S, Gascuel O. 2003. A simple, fast, and accurate algorithm to estimate large phylogenies by maximum likelihood. Systematic Biology 52:696–704. DOI:10.1080/10635150390235520.

Harada Y, Hosoiri Y, Kuroda R. 2004. Isolation and evaluation of dextral-specific and dextralenriched cDNA clones as candidates for the handedness-determining gene in a freshwater gastropod, *Lymnaea stagnalis*. Development Genes and Evolution 214:159–169. DOI:10.1007/s00427-004-0392-6.

Hewitt GM. 1999. Post-glacial re-colonization of European biota. Biological Journal of the Linnean Society 68:87–112. DOI:10.1111/bij.1999.68.issue-1-2.

Hewitt GM. 2000. The genetic legacy of the quaternary ice ages. Nature 405:907–913. DOI:10.1038/35016000.

Hierck BP, Witte B, Poelmann RE, Gittenberger-de Groot AC, Gittenberger E. 2005. Chirality in snails is determined by highly conserved asymmetry genes. Journal of Molluscan Studies 71:192–195. DOI:10.1093/mollus/eyi023.

Hijmans RJ, Cameron SE, Parra JL, Jones PG, Jarvis A. 2005. Very high resolution interpolated climate surfaces for global land areas. International Journal of Climatology 25:1965–1978. DOI:10.1002/(ISSN)1097-0088.

Hoso M, Kameda Y, Wu SP, Asami T, Kato M, Hori M. 2010. A speciation gene for left-right reversal in snails results in anti-predator adaptation. Nature Communication 1:133. DOI:10.1038/ncomms1133.

IUCN. 2015. The IUCN Red List of Threatened Species. Version 2015-4. www.iucnredlist.org.

Koene J, Cosijn J. 2012. Twisted sex in an hermaphrodite: Mirror-image mating behaviour is not learned. Journal of Molluscan Studies 78:308–311. DOI:10.1093/mollus/eys016.

Kuroda R. 2014. How a single gene twists a snail. Integrative Comparative Biology 54:677–687. DOI:10.1093/icb/icu096.

Kuroda R, Endo B, Abe M, Shimizu M. 2009. Chiral blastomere arrangement dictates zygotic left-right asymmetry pathway in snails. Nature 462:790–794. DOI:10.1038/nature08597.

Librado P, Rozas J. 2009. DnaSP v5: A software for comprehensive analysis of DNA polymorphism data. Bioinformatics 25:1451–1452. DOI:10.1093/bioinformatics/btp187.

Liu MM, Davey JW, Banerjee R, Han J, Yang F, Aboobaker A, Blaxter ML, Davison A. 2013. Fine mapping of the pond snail left-right asymmetry (chirality) locus using RAD-Seq and Fibre-FISH. PLoS ONE 8:e71067. DOI:10.1371/journal.pone.0071067.

Monaghan MT, Wild R, Elliot M, Fujisawa T, Balke M, Inward DJ, Lees DC, Ranaivosolo R, Eggleton P, Barraclough TG, Vogler AP. 2009. Accelerated species inventory on Madagascar using coalescent-based models of species delineation. Systematic Biology 58:298–311. DOI:10.1093/sysbio/syp027.

Nieberding C, Libois R, Douady CJ, Morand S, Michaux JR. 2005. Phylogeography of a nematode (*Heligmosomoides polygyrus*) in the Western Palearctic region: Persistence of northern cryptic populations during ice ages? Molecular Ecology 14:765–779. DOI:10.1111/j.1365-294X.2005.02440.x.

Nylander JAA. 2004. MrModeltest v2. Program distributed by the author.

Oksanen J, Blanchet FG, Kindt R, Legendre P, Minchin PR, O'Hara RB, Simpson GL, Solymos P, Stevens MHH, Wagner H. 2012. vegan: Community ecology package. R package version 2.0-4.

Oliverio M, De Matthaeis E, Hallgass A. 1992. Genetic divergence between Italian populations of *Marmorana* (*Ambigua*) (Gastropoda, Pulmonata, Helicidae). Lavori della Società Italiana di Malacologia 24:225–248.

Oliverio M, Digilio MC, Versacci P, Dallapiccola B, Marino B. 2010. Shells and heart: Are human laterality and chirality of snails controlled by the same maternal genes? American Journal of Medical Genetics, Part A 152A:2419–2425. DOI:10.1002/ajmg.a.v152a:10.

Oliverio M, Mariottini P. 2001. A molecular framework for the phylogeny of *Coralliophila* and related muricoids. Journal of Molluscan Studies 67:9. DOI:10.1093/mollus/67.2.215.

Padial JM, Miralles A, De la Riva I, Vences M. 2010. The integrative future of taxonomy. Frontiers in Zoology 7:16. DOI:10.1186/1742-9994-7-16.

Paradis E. 2010. Pegas: An R package for population genetics with an integrated-modular approach. Bioinformatics 26:419–420. DOI:10.1093/bioinformatics/btp696.

Podnar M, Mayer W, Tvrtkovic N. 2005. Phylogeography of the Italian wall lizard, *Podarcis sicula*, as revealed by mitochondrial DNA sequences. Molecular Ecology 14:575–588. DOI:10.1111/j.1365-294X.2005.02427.x.

Pons J, Barraclough TG, Gomez-Zurita J, Cardoso A, Duran DP, Hazell S, Kamoun S, Sumlin WD, Vogler AP. 2006. Sequence-based species delimitation for the DNA taxonomy of undescribed insects. Systematic Biology 55:595–609. DOI:10.1080/10635150600852011.

Posada D, Crandall KA. 1998. MODELTEST: Testing the model of DNA substitution. Bioinformatics 14:817–818. DOI:10.1093/bioinformatics/14.9.817.

Posada D, Crandall KA. 2001. Selecting the best-fit model of nucleotide substitution. Systematic Biology 50:580–601. DOI:10.1080/106351501750435121.

Puillandre N, Lambert A, Brouillet S, Achaz G. 2012a. ABGD, Automatic Barcode Gap Discovery for primary species delimitation. Molecular Ecology 21:1864–1877. DOI:10.1111/j.1365-294X.2011.05239.x.

Puillandre N, Modica MV, Zhang Y, Sirovich L, Boisselier MC, Cruaud C, Holford M, Samadi S. 2012b. Large-scale species delimitation method for hyperdiverse groups. Molecular Ecology 21:2671–2691. DOI:10.1111/j.1365-294X.2012.05559.x.

R Development Core Team. 2014. R: A language and environment for statistical computing. Vienna, Austria: R Foundation for Statistical Computing. Available: http://www.R-project.org. Accessed Feb 2015 6.

Rambaut A, Suchard MA, Xie D, Drummond AJ. 2014. Tracer, version 1.6. Available: http://beast.bio.ed.ac.uk/Tracer. Accessed Feb 2015 1.

Ronquist F, Teslenko M, van der Mark P, Ayres DL, Darling A, Höhna S, Larget B, Liu L, Suchard MA, Huelsenbeck JP. 2012. MrBayes 3.2: Efficient bayesian phylogenetic inference and model choice across a large model space. Systematic Biology 61:539–542. DOI:10.1093/sysbio/sys029.

Schilthuizen M, Davison A. 2005. The convoluted evolution of snail chirality. Naturwissenschaften 92:504–515. DOI:10.1007/s00114-05-0045-2.

Schilthuizen M, Haase M, Koops K, Looijestijn SM, Hendrikse S. 2012. The ecology of shell shape difference in chirally dimorphic snails. Contributions to Zoology 81:95–101.

Schilthuizen M, Lombaerts M. 1994. Population-structure and levels of gene flow in the Mediterranean land snail *Albinaria corrugata* (Pulmonata, Clausiliidae). Evolution 48:577–586. DOI:10.2307/2410470.

Servedio MR, van Doorn GS, Kopp M, Frame AM, Nosil P. 2011. Magic traits in speciation: "magic" but not rare? Trends in Ecology & Evolution 26:389–397. DOI:10.1016/j.tree.2011.04.005.

Shimizu K, Iijima M, Setiamarga DHE, Sarashina I, Kudoh T, Asami T, Gittenberger E, Endo K. 2013. Left-right asymmetric expression of dpp in the mantle of gastropods correlates with asymmetric shell coiling. EvoDevo 4:15. DOI:10.1186/2041-9139-4-15.

Shimizu K, Sarashina I, Kagi H, Endo K. 2011. Possible functions of Dpp in gastropod shell formation and shell coiling. Develpment Genes Evolution 221:59–68. DOI:10.1007/s00427-011-0358-4.

Srivathsan A, Meier R. 2011. On the inappropriate use of Kimura-2-parameter K2P divergences in theDNA-barcoding literature. Cladistics. DOI:10.1111/j.1096-0031.2011.00370.x.

Sturtevant AH. 1923. Inheritance of direction of coilling in *Lymnaea*. Science 58:269–270. DOI:10.1126/science.58.1501.269.

Swofford DL. 1993. Phylogenetic Analysis Using Parsimony (PAUP). Version 3.1.1. Champaign: University of Illinois.

Tamura K, Peterson D, Peterson N, Stecher G, Nei M, Kumar S. 2011. MEGA5: Molecular evolutionary genetics analysis using maximum likelihood, evolutionary distance, and maximum parsimony methods. Molecular Biology and Evolution 28:2731–2739. DOI:10.1093/molbev/msr121.

Tanzler R, Sagata K, Surbakti S, Balke M, Riedel A. 2012. DNA barcoding for community ecology - How to tackle a hyperdiverse, mostly undescribed melanesian fauna. PLoS One 7: e28832. DOI:10.1371/journal.pone.0028832.

Tomaz D, Guiller A, Clarke B. 1996. Extreme divergence of mitochondrial DNA within species of pulmonate land snails. Proceedings of the Royal Society of London B 263:363–368. DOI:10.1098/rspb.1996.0056.

Ueshima R, Asami T. 2003. Evolution: Single-gene speciation by left–right reversal. Nature 425:679–679. DOI:10.1038/425679a.

Vigna Taglianti A, Audisio PA, Belfiore C, Biondi M, Bologna MA, Carpaneto GM, De Biase A, De Felici S, Piattella E, Racheli T, Zapparoli M, Zoia S. 1992. Riflessioni di gruppo sui corotipi fondamentali della fauna W-paleartica ed in particolare italiana. Biogeographia 16:159–179.